

Adaptive highlights stencils for modeling of multi-axial BRDF anisotropy

An alternative to analytical anisotropic BRDF modeling

Jiří Filip¹ · Michal Havlíček¹ · Radomír Vávra^{1,2}

© Springer-Verlag Berlin Heidelberg 2015

Abstract Directionally dependent anisotropic material appearance phenomenon is widely represented using bidirectional reflectance distribution function (BRDF). This function needs in practice either reconstruction of unknown values interpolating between sparse measured samples or requires data fidelity preserving compression forming a compact representation from dense measurements. Both properties can be, to a certain extent, preserved by means of analytical BRDF models. Unfortunately, the number of anisotropic BRDF models is limited, and moreover, most require either a demanding iterative optimization procedure dependent on proper initialization or the user setting parameters. Most of these approaches are challenged by the fitting of complex anisotropic BRDFs. In contrast, we approximate BRDF anisotropic behavior by means of highlight stencils and derive a novel BRDF model that independently adapts such stencils to each anisotropic mode present in the BRDF. Our model allows for the fast direct fitting of parameters without the need of any demanding optimization. Furthermore, it achieves an encouraging, expressive visual quality as compared to rival solutions that rely on a similar number of parameters. We thereby ascertain that our method represents a promising approach to the analysis and modeling of complex anisotropic BRDF behavior.

Electronic supplementary material The online version of this article (doi:10.1007/s00371-015-1148-1) contains supplementary material, which is available to authorized users.

✉ Jiří Filip
filipj@utia.cas.cz

¹ Institute of Information Theory and Automation, ASCR, Pod Vodárenskou věží 4, 182 08 Prague 8, Czech Republic

² Faculty of Information Technology, Czech Technical University, Prague, Czech Republic

Keywords Anisotropic · Highlight · Stencils · BRDF · Model

1 Introduction

Each material surface reflects a certain portion of incident light. Generally, the light scatters in the material structure and leaves it either as reflectance or as transmittance. If we restrict the surface in being opaque, light is reflected in directions constrained by a hemisphere whose pole intersects with the surface normal.

The distribution of the differential reflected radiance dL for incident irradiance dE is a four-dimensional bidirectional reflectance distribution function (BRDF) [14]

$$B(\theta_i, \varphi_i, \theta_v, \varphi_v) = \frac{dL(\theta_v, \varphi_v)}{dE(\theta_i, \varphi_i)} = \frac{dL(\theta_v, \varphi_v)}{L(\theta_i, \varphi_i) \cos \theta_i d\omega_i}, \quad (1)$$

where parameterization of illumination $\omega_i = [\theta_i, \varphi_i]$ and viewing $\omega_v = [\theta_v, \varphi_v]$ directions is illustrated in Fig. 1. This equation defines anisotropic BRDF, i.e., having variable values when mutually fixed illumination and viewing directions are rotated around the material normal. When these values are constant, the BRDF is considered isotropic and defined as only a three-dimensional function. Figure 1 right illustrates a 4D BRDF unfolded into 2D image, i.e., into individual BRDF subsets for increasing elevation illumination/view angles from 0° to 75° are shown side by side vertically/horizontally.

Figure 2 shows effect of anisotropic highlights when compared to isotropic highlights only; this example clearly demonstrates importance of modeling a full 4D anisotropic BRDF for highly anisotropic samples.

A BRDF has three important properties namely reciprocity, energy conservation, and non-negativity. All of them are based on physical principles of light interaction with the surface. Helmholtz reciprocity states that illumination and viewing directions can be swapped without any effect on

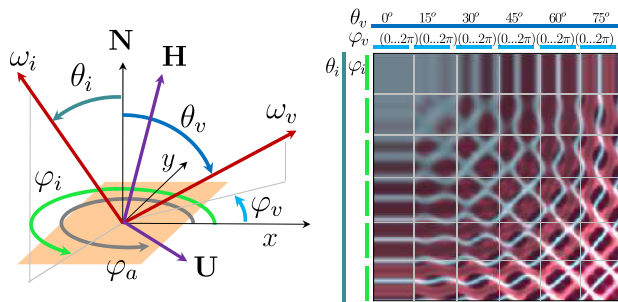


Fig. 1 BRDF angular parameterization (left) and 4D BRDF unwrapping into 2D image (right) used within this paper

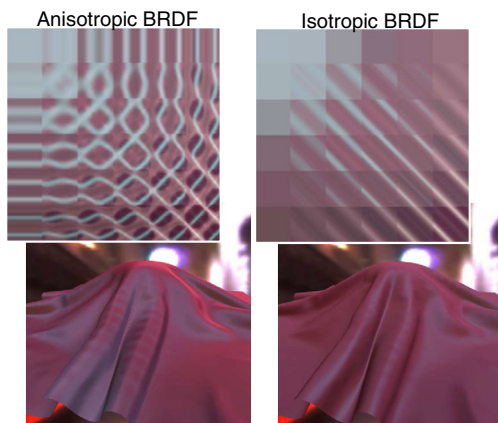


Fig. 2 Importance of anisotropic appearance. A comparison between BRDFs and rendering of the anisotropic material *fabric106* (left) and the same material with its anisotropic behavior removed (right) on 3D geometry in global illumination

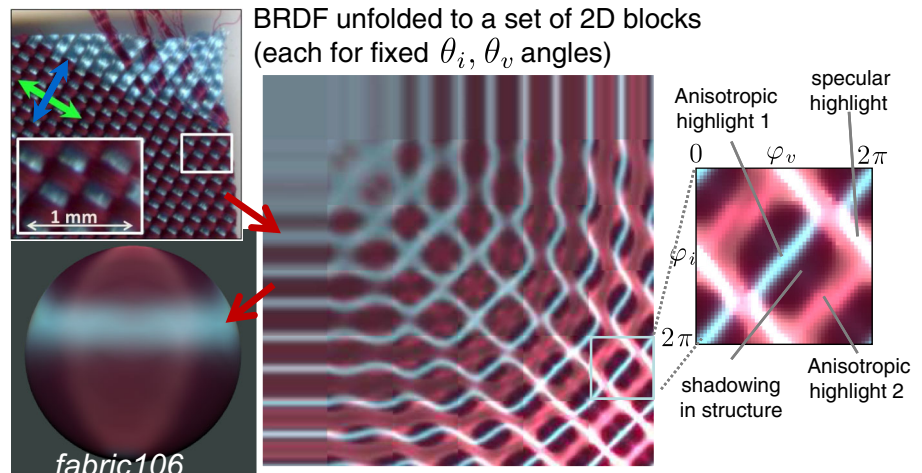
the BRDF value. Energy conservation specifies that the total reflected energy cannot be greater than the sum of incoming energy. Non-negativity ensures positive distribution values.

An example of a BRDF having two distinct anisotropic modes, i.e., unique highlights, is shown in Fig. 3. A detailed analysis of the selected subset reveals two different anisotropic highlights corresponding to two threads occurring in the material. While the brighter blue anisotropic highlight (AHL1) corresponds to a visually dominant thread, the less bright red one (AHL2) belongs to a less dominant thread. Note also increased intensity at specular direction, i.e., when $|\varphi_i - \varphi_v| \approx \pi$. Within this paper we denote individual anisotropic highlights caused by different structure elements as anisotropy modes.

A main goal of BRDF modeling has been to develop a compact representation of sparsely measured BRDF data. In contrast to BRDF compression, the goal of BRDF models is, not only to compress measured samples, but also to predict values between the measured samples in order to approximate unknown data. The primary aim in optimal BRDF model development is in finding a compact parametric representation that can faithfully describe the dominant behavior of the BRDF. Moreover, such a model should be ideally physically plausible, reciprocal and energy-conserving, as well as easy to implement in graphics hardware for a higher rendering efficiency.

A typical solution relies on an iterative algorithm that monotonically converge to a correct solution. However, this process is often very time demanding, and its results depend on a proper setting of initial values. The main contributions of this paper are (1) the analysis of typical behavior of anisotropic highlights using highlights stencils and (2) a new approach to BRDF modeling based on the direct fitting of these stencils to individual anisotropic highlights (related to a specific structure part of material surface). Our approach is not based on the global fitting of reflectance lobes paramete-

Fig. 3 An example of anisotropic BRDF behavior of *fabric106*. Major visual features are shown in BRDF subset obtained for fixed elevation angles. It illustrates azimuthally dependent BRDF behavior



ters, but instead approximates individual modes of anisotropy independently, i.e., always using just a subset of BRDF. Therefore, it allows for the very fast identification of parameters without them needing to be initialized. Moreover, many parameters are intuitive, which thus allows for an efficient editing of fitted BRDFs.

The contents of the paper are as follow: In Sect. 2, we set our work in the context of BRDF modeling research. Section 3 describes the proposed BRDF model and Sect. 4 shows achieved results on a set of BRDFs. Section 5 discusses the method's pros and cons, while Sect. 6 concludes the paper.

2 Prior work

In the past, BRDF measurements were approximated by several methods that exploited properties of typical BRDFs such as reciprocity, smoothness, location and shape of specular reflection, etc. We can roughly divide BRDF models into two categories. While empirical models compromise accuracy and physical plausibility in order to achieve a low number of parameters and thus faster evaluation, the physically derived models offer higher descriptive qualities, albeit at the cost of computational demands.

Most empirical models represent BRDF by means of a specific type of reflectance function expressing a mutual relationship between the directions to illumination φ_i , viewer φ_v , and the normal direction \mathbf{N} (see Fig. 1). The empirically derived models are usually based on a very simple formula with several adjustable parameters designed to fit a certain class of reflectance functions. The most common is a model by Phong [16] and its more practical modification by Blinn [3]. A generalization of the Phong model based on cosine lobes was introduced by Lafortune et al. [10]. A simplified physically plausible anisotropic reflectance model based on Gaussian distribution of micro-facets was presented by Ward [23]. The model has the necessary bidirectional characteristics, and all four of its parameters have physical meaning; therefore, it can be fitted independently to measured BRDF data to produce a physically valid reflectance function that fulfills reciprocity and energy conservation. A model by Schlick [21] stands halfway between empirical and theoretical models. Ashikhmin and Shirley [1] extended the Phong-based specular lobe, made this model anisotropic, and incorporated a Fresnel behavior while attempting to preserve the physical plausibility and computational simplicity of the initial model.

In contrast, physically motivated models are designed to represent some known physical phenomena; therefore, individual parameters or fitted functions are related to properties of real materials. Torrance and Sparrow's [22] pioneer model represents a surface by the distribution of vertical

V grooves, perfectly specular micro-facets. This model was later enhanced and introduced to the computer graphics community by Cook and Torrance [4] and further extended for more accurate and stable fitting by a shifted gamma micro-facet distribution in [2]. The micro-facet models are typically based on a combination of Fresnel, facet distribution, and shadowing/masking functions. It was shown [8] that the distribution and masking functions can be effectively used for modeling of anisotropic behavior. Such an anisotropic extension of the Cook–Torrance model was recently introduced by Kurt et al. [9]. This model is based on a normalized micro-facet distribution function, is physically plausible, and is designed to be more advantageous for data fitting and real-time rendering. Dupuy et al. [5] proposed an approach to the efficient fitting of facets distributions based on solving an eigenvector problem relying solely on backscattering samples. Although this method provides a very convenient way of the authoring of estimated distribution roughness properties and can fit an anisotropic BRDF in 20 s, its final accuracy depends, due to its principle, on the density of BRDF measurements in a backscattering direction. Therefore, the fitting quality can be limited especially for complex multi-axial anisotropic BRDFs.

The most complete and complex BRDF model was proposed by He et al. [7]. Although it accounts for many physical phenomenon involved in light reflection on rough surfaces such as polarization, diffraction, conductivity, and subsurface scattering, it cannot correctly represent anisotropic BRDFs. Nayar and Oren [13] extended Torrance and Sparrow [22] to modeling of surface roughness using Lambertian facets. An efficient isotropic BRDF model based on rational function was recently proposed by Pacanowski et al. [15]. The model uses reduced Rusinkiewicz parameterization [19], relies on a compact set of parameters, and its extension allows limited modeling of anisotropic effects.

Another physically motivated appearance model by Sadeghi et al. [20] extending original work of Poulin and Fournier [17], is based on the physics of light scattering in cylindrical threads of fibers and achieves anisotropy by the application of a user-defined weaving pattern of two threads together with parameters of their reflectance model. A drawback of this model is the complicated application of parameter optimization techniques; therefore, the derivation of appropriate parameters of individual threads is left completely to users and their experience.

Our approach is closely related to anisotropic empirical models, yet instead of the iterative fitting of a global reflectance, it directly represents anisotropic phenomena caused by individual directionally dependent structure elements. This results in a fast and robust fitting to BRDF data using a compact parameter set comparable in size with competing models and with minimal user input requirements.

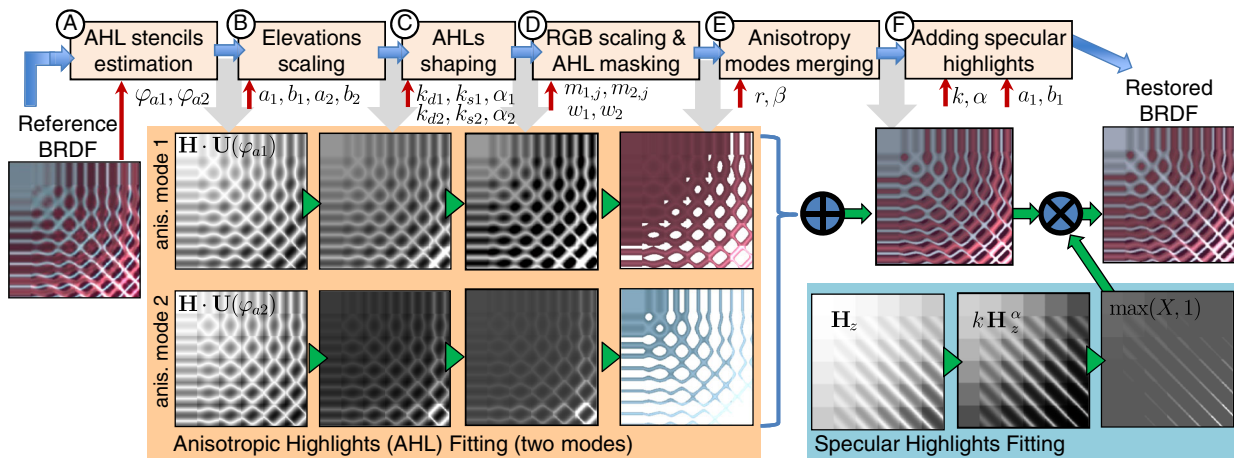


Fig. 4 Overall scheme of the proposed BRDF model

3 The proposed BRDF model

The proposed model is based on the independent modeling of anisotropic modes in given materials, e.g., individual threads in the case of fabrics or fibers in the case of wood. Although the proposed model is not limited to modeling of two anisotropy modes only (see Sect. 5.1), we restrict ourselves so for clarity reasons in this section.

3.1 Model description

An overall scheme of the proposed model is outlined in Fig. 4. We describe individual parts of the model in the following sections with letters related to those in the scheme. Note that the products of the model dependent on incoming and outgoing directions are denoted by capital letters, while scalar parameter values are in lowercase or Greek letters.

3.1.1 Anisotropic highlights prediction

Our method starts with the representation of main anisotropy axes using highlights stencils. First, we automatically detect the azimuthal location of anisotropic highlights (i.e., φ_a of each mode) by analyzing cross-sections of a BRDF for fixed elevation illumination direction ($\theta_i = 75^\circ, \varphi_i = 0^\circ, \theta_v \approx 60^\circ$). As we expect two modes of anisotropy, we are merely looking for two peaks in azimuthal angles $[0 - 2\pi)$ (for n -modal anisotropy we would look for n peaks). Their location determines the direction of anisotropy φ_a as shown in Fig. 5.

Then the locations of anisotropic highlights can be predicted on directional surface elements, laying in planes orthogonal to the bisector (often denoted as half-way direction $\mathbf{H} = \frac{\omega_i + \omega_v}{\|\omega_i + \omega_v\|}$) of directions of incidence and reflectance as proposed in [12]. Therefore, the anisotropic highlights can be predicted [18] at directions of the bisector which are

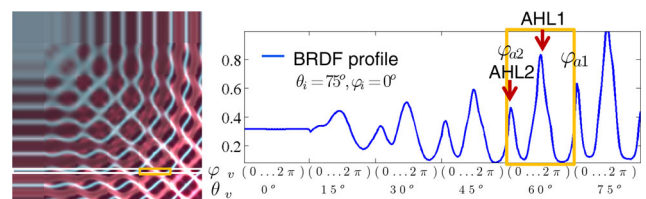


Fig. 5 Detection of anisotropic directions φ_{a1} and φ_{a2} from 1D BRDF profile (material *fabric106*). Only data in yellow frame are needed

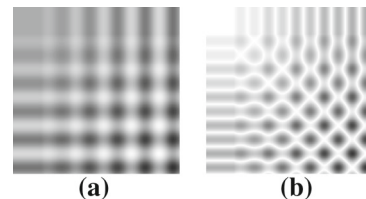


Fig. 6 Highlights stencil: predicting of anisotropic highlight location **b** using a dot-product of half-way direction \mathbf{H} and the detected direction of anisotropy $\mathbf{U} = [\sin \varphi_a, \cos \varphi_a, 0]$, for $\varphi_a = 0^\circ$

orthogonal to the detected anisotropy axis of the material $\mathbf{U} = [\sin \varphi_a, \cos \varphi_a, 0]$ (see Fig. 1). Thus, the highlights stencils can be expressed as:

$$F(\varphi_a) = 1 - |\mathbf{H} \cdot \mathbf{U}(\varphi_a)|$$

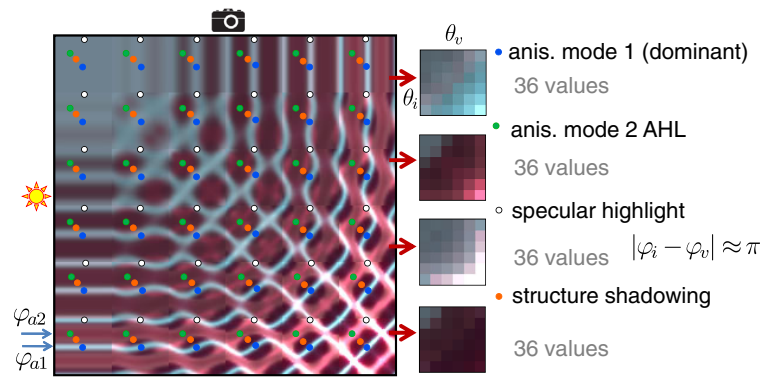
$$\mathbf{U}(\varphi_a) = [\sin \varphi_a, \cos \varphi_a, 0]. \tag{2}$$

Figure 6 shows the application of the highlights stencil function F for prediction of anisotropic highlights locations across many incidence and reflectance directions for a given φ_a .

3.1.2 Elevation-dependent scaling

The obtained stencil functions F for each mode ($\varphi_{a1}, \varphi_{a2}$) have to be scaled to reflect illumination/view-dependent intensity present in the to-be-fitted BRDF. Therefore, the

Fig. 7 Data collection for model fitting: sampling of anisotropic highlights (blue and green dots), specular highlights (white dots), and shadowed areas (orange dots) values



anisotropic highlight for respective modes is sampled once at each view/illumination elevation angle across the entire BRDF in order to acquire its elevation-dependent intensity (see blue and green dots in Fig. 7). This 2D function representing elevation-dependent intensity is approximated by parameters a, b and applied to scale functions $F(\varphi_{a1}), F(\varphi_{a2})$ as follows:

$$\begin{aligned} E_1 &= F(\varphi_{a1}) \left(a_1 + \frac{b_1}{\cos \theta_i \cos \theta_v} \right) \\ E_2 &= F(\varphi_{a2}) \left(a_2 + \frac{b_2}{\cos \theta_i \cos \theta_v} \right) \end{aligned} \quad (3)$$

3.1.3 Anisotropic highlights shape fitting

The shape of the predicted anisotropic highlights in functions E_1 and E_2 is further adapted to the BRDF data, due to its simplicity, by a variant of the Blinn–Phong model $k_d + k_s (N \cdot H)^\alpha$ [3]. To this end, we fit model parameters (diffuse and specular parameters k_d, k_s , and specular exponent α) for each mode (further discriminated by numbers 1 and 2) using the luminance of the to-be-fitted BRDF and the function E .

$$\begin{aligned} L_1 &= k_{d1} + k_{s1} E_1^{\alpha_1} \\ L_2 &= k_{d2} + k_{s2} E_2^{\alpha_2}. \end{aligned} \quad (4)$$

To account for areas of anisotropic highlights only in our fitting, we generate support masks M around each mode's highlight as shown in Fig. 4d. The mask for each mode includes only a surrounding along its anisotropic highlights centers. It identifies mode's support samples for a proper k_d, k_s, α fitting and for further modes merging. As the function $\mathbf{H} \cdot \mathbf{U}$ represents a modulated sinusoidal function (see Fig. 6a), the masks can be obtained using a thresholding of function $1 - |\mathbf{H} \cdot \mathbf{U}(\varphi_a)| < w$, where w relates to the width of specular highlight. The support mask M can be either binary or smooth as follows:

$$M(\varphi_a, w) = \begin{cases} 1 & x \leq w - d_w \\ 0 & x \geq w + d_w \\ f(x) & w - d_w < x < w + d_w, \end{cases}$$

where $x = 1 - |\mathbf{H} \cdot \mathbf{U}(\varphi_a)|$, and $f(x)$ is a smoothstep function $f(x) = y^2(3 - 2y)$ where $y = \frac{x - w + d_w}{2d_w}$. We have chosen this function as it is a part of OpenGL shading language, and thus directly supported by GPUs. The best results were obtained with parameter d_w in interval $0.1w - 0.2w$.

3.1.4 Color scaling and highlights masking

Finally, color information is introduced by the scaling of a fitted luminance value L using 3 RGB color parameters m_i .

$$\begin{aligned} T_{1i} &= m_{1i} \cdot \max(0, L_1) \\ T_{2i} &= m_{2i} \cdot \max(0, L_2), \end{aligned} \quad (5)$$

where i stands for color channel index (R,G,B) and maximum guarantees BRDF non-negativity. The color parameters m_i are obtained by a linear fitting of the luminance function L to values of individual color channels in the BRDF.

By combining Eqs. (2), (3), (4), and (5) we obtain the final equation representing a contribution of a single anisotropy mode

$$T_i = m_i \cdot \max(0, k_d + k_s \left[(1 - |\mathbf{H} \cdot \mathbf{U}(\varphi_a)|) \left(a + \frac{b}{\cos \theta_i \cos \theta_v} \right) \right]^\alpha). \quad (6)$$

3.1.5 Anisotropic modes merging

At this point each mode is represented by its support contours M and the intensity in each color channel (6). The information from both modes have to be blended and the missing parts of the BRDF filled. Dark reflectance values not belonging to highlight areas correspond to what we call “background” color related to shadowing caused by elements in the material structure. Therefore, we pick the darkest measured value for each illumination/view elevation in BRDF and compute the linear scaling factor r ($r < 1$) between the color intensities of the “background” and the average color of the less dominant mode. Note that the mean color of the less dominant

mode can be effectively substituted by the respective color parameter m_{2i} .

The modes merging then works as follows. First background is combined with the less bright mode using

$$P_i = (1 - M_2) \cdot r \cdot m_{2i} + M_2 \cdot T_{2i}. \tag{7}$$

This product P is further combined with the dominant mode using

$$B_i = (1 - M_1) \cdot P_i + M_1 \cdot [(1 - \beta)T_{1i} + \beta T_{2i}], \tag{8}$$

where parameter β controls the final contributions of both modes at their intersections. If $\beta = 0$, the upper mode is considered fully opaque, while its increasing value introduces its translucency. This formula can be extended when more than two modes are applied. The Eq. (8) can be rewritten as a linear combination of background and modes contributions using

$$B_i = (1 - M_1)(1 - M_2) \cdot r \cdot m_{2i} + M_1(1 - \beta) \cdot T_{1i} + [(1 - M_1)M_2 + M_1\beta] \cdot T_{2i}. \tag{9}$$

If one would want to use only binary support masks the final equation translates to

$$B_i = \begin{cases} (1 - \beta)T_{1i} + \beta T_{2i} & M_1 = 1 \\ P_i & M_1 = 0, M_2 = 0 \\ T_{2i} & M_1 = 0, M_2 = 1 \end{cases}$$

Although this equation is simpler than (9) we recommend smooth support mask as they avoid possible visual artifacts caused by sharp transitions between the modes.

3.1.6 Specular highlights fitting

As the majority of the materials also have a significant specular contribution on the top of the anisotropic highlights represented by modified stencil functions, we approximate this behavior by the modification of the z -coordinate of a half-vector direction H_z . As the dominant (brighter) mode represents the main contribution to the specular highlight, we approximate specular highlights elevation-dependency by means of its intensity, i.e., using parameters a_1, b_1 for introduction of specular elevation dependency, while the shape of specular highlights is controlled using the modified Blinn–Phong model again [3] ($k(N \cdot H)^\alpha$). Specular highlights are sampled similarly as anisotropic highlights, i.e., one sample for each combination of illumination/viewing elevation angles. Additionally, we also sample the dark-

est value for each elevations combinations (see white and orange dots in Fig. 7). This data and the elevation intensity-compensated function H_z are used to fit the model’s parameters.

Finally, the specular contribution is added to our model as follows:

$$B_{S,i} = B_i \cdot \max \left[1, k \cdot H_z^\alpha \cdot \left(a_1 + \frac{b_1}{\cos \theta_i \cos \theta_v} \right) \right]. \tag{10}$$

Maximum function prevents the specular factor to decrease the final reflectance intensity.

3.2 Implementation details

Parameters Our model has ten parameters per anisotropy mode: anisotropic axis direction φ_a , width of mode support w , elevation-dependent intensity fitting a, b , color scaling $3 \times m$, and parameters controlling shape of the highlight (k_d, k_s, α). Additionally, it has four global parameters: blending factor β , background scaling factor r , and specular highlight modeling parameters k, α . A comparison of parameters count required by several anisotropic BRDF modeling approaches is given in Table 1.

Data fitting The direct parameters estimation we applied is data driven and avoids iterative optimization dependent on initial values; therefore, it significantly lessens the risk of being captured in a local minimum. As no iterative optimization is applied in our method, the proposed fitting is very fast. It takes only 3 s using a single core of Intel Core i7. We used standard MATLAB functions fit for parameter a, b estimation and nlinfit for nonlinear parameters k_s, k_d, α estimation.

A minimal variant of our method requires only $4 \times 36 = 144$ color BRDF samples (see Fig. 7) to estimate its parameters; however, an optimal shape reproduction of specular and anisotropic highlights requires more samples along these features. Note that although locations of samples shown in Fig. 7 are angularly uniform, we assume that our method would be able to learn its parameters also from scattered BRDF samples of reasonable density. This can be done either by taking the closest value, or by interpolating/extrapolating possibly missing values at some elevations.

The adjustment of three parameters is up to the user; although, their default values work fairly well. Blending

Table 1 Number of parameters of individual tested models

Parameters	Kurt et al. [9]	Sadeghi et al. [20]	Proposed
Global	3	0	4
Per mode/lobe	7	10 min	10
Total (2 th./lob.)	17	20 min	24

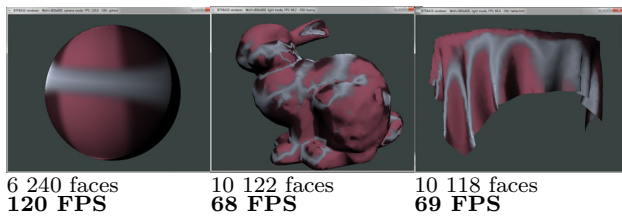


Fig. 8 Performance of our GPU rendering implementation shown on three objects and material *fabric106* at resolution 800×600 pixels

factor β controls model behavior at directions of modes intersections. The typical value is 0, although it can be increased up to 1 in relation to the dominant mode's translucency. Support of the anisotropic highlights is controlled by their width parameter w , where 0 represents extremely wide, whereas 1, extremely narrow threads. Although parameter w is currently user-defined in our implementation, it can possibly be estimated from the width of anisotropic highlights in the to-be-fitted BRDF. Typical values are $w_1 = 0.7$ for the dominant mode and $w_2 = 0.6$ for the second mode as it often has wider highlight support.

Note that the model parameters for all materials in the paper and supplemental material were obtained automatically without any manual intervention. Only parameters β , w_1 , w_2 were slightly adjusted for each material. Please see the list of all model parameter values for each material in the supplemental material. The model's performance can be further improved by the user slightly tuning it.

GPU rendering We implemented rendering of the proposed model on GPU. Our OpenGL implementation runs on a mobile GPU NVIDIA Quadro K1000M with typical rendering speeds between 60–120 frames per second (FPS) for window resolution 800×600 pixels and meshes of ≈ 10 k polygons (see Fig. 8). Length of our shader function restoring BRDF from its parameters is only 40 lines as shown in the supplementary material.

4 Experiments

4.1 Test datasets

As the number of publicly available anisotropic BRDFs is limited, we turned to the UTIA BRDF Database¹ [6] as the only source of a reasonable number of different types of anisotropic BRDF measurements. This database contains 150 BRDF out of which over 50 exhibit some aspect of anisotropy. The BRDFs are stored in a 32-bit float HDR format, and their angular resolution is 15° in elevations and 7.5° in azimuthal angles. We tested our model on 14 BRDFs

exhibiting various types of anisotropy (13 types of fabric, 1 wood).

4.2 Results

We fitted our model to 14 tested BRDFs. Figure 9 shows the results for four of them. The figure compares a reference BRDF measurement with its reconstruction using two physically based anisotropic BRDF models by Kurt et al. [9] and Sadeghi et al. [20]. In the Kurt model we fitted two lobes each using dedicated parameters k_s , k_d for each RGB channel, while lobe parameters f_0 , m_x , m_y , α were fitted to luminance values only. The Sadeghi model was fitted by a parametrization of two modes as suggested in the paper. We included difference images between reference and reconstructed BRDFs as well as mean difference computational values using ΔE /RMSE/PSNR [dB]/SSIM/VDP2 metrics. The results demonstrate an encouraging performance in our model especially when compared with the competing methods.

This is supported by a comparison of a BRDFs rendering on a frontally illuminated sphere as shown in Fig. 10, where our model shows a promising performance in the capturing of most anisotropic features.

Finally, Fig. 11 presents side-by-side renderings of reference BRDF and its reconstruction using the proposed model for all 14 tested BRDFs in a global illumination environment. The remaining results including parameters listing are shown in the supplementary material.

5 Discussion

5.1 Advantages

A notable advantage of our model is a fast and reasonably robust fitting procedure without the need for demanding optimization.

As our approach is based on the direct prediction of individual anisotropic modes, it is well suited to the interactive editing of BRDFs, perhaps utilized in future intuitive GUI. Figure 12 illustrates several straightforward editing examples—change of mode's anisotropy axes using modification of the estimated angles φ_a (a, b), width of anisotropic highlight by change of parameter w (c), and mode's color by swapping the first two color channels between the modes, i.e., parameters m_i (d). Furthermore, we also release our example GPU shader compatible for BRDFexplorer² and show the *fabric106* material lobes together with the rapid editing example Fig. 13.

¹ <http://btf.utia.cas.cz>.

² <http://www.disneyanimation.com/technology/brdf.html>.

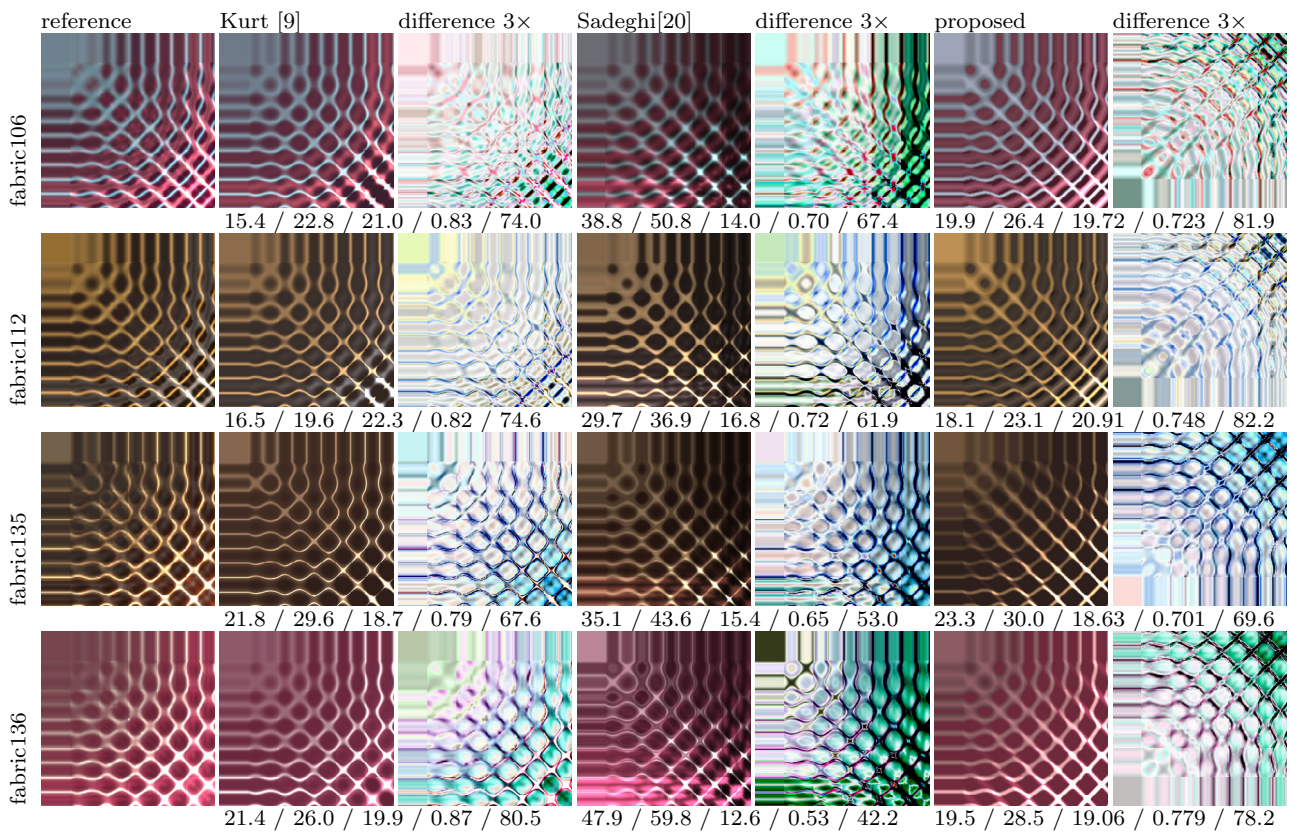


Fig. 9 A comparison of reference BRDF and its reconstructions using three compared models for four BRDFs of anisotropic fabric materials. Included are difference images (scaled 3x) and results of ΔE /RMSE/PSNR [dB]/SSIM/VDP2 metrics

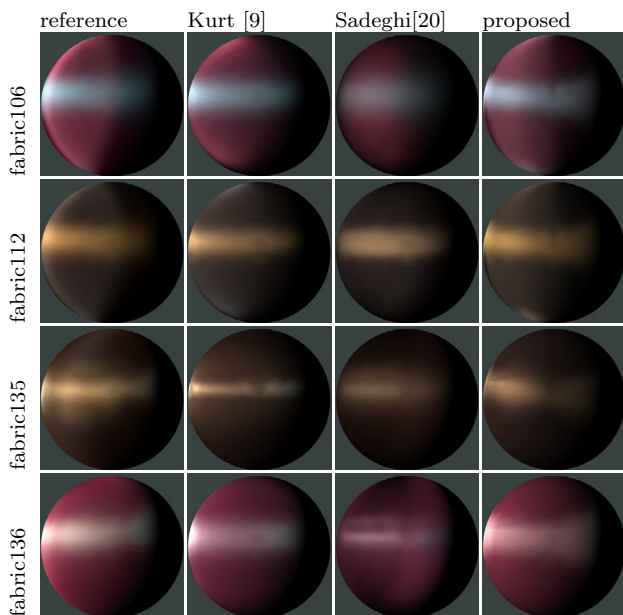


Fig. 10 A rendering comparison of reference BRDF and its reconstructions, on sphere illuminated by point light from left, using three compared BRDF models

Our anisotropic highlights prediction algorithm can also be applied to BRDF retro-reflection modeling as demonstrated in Fig. 14. The retro-reflective highlights can be predicted merely by modifying azimuthal illumination angles $\varphi_i = \varphi_i + \pi$ prior to half-way direction \mathbf{H} computation for highlights stencils predictions.

Our current implementation is not limited to the fitting of two anisotropy modes only (e.g., two fabric threads), but can be extended. To show such a functionality, we experimented with BRDF having three anisotropic axes. As such BRDFs are quite rare in the real-world and as so far no such BRDF measurements are publicly available, we created an artificial one by combining two BRDFs of *fabric106* (2 modes) and *fabric111* (1 mode) as shown in Fig. 15. Note that the third mode was introduced by the second BRDF's anisotropic highlight rotation for 45° and its application in a green color channel only. The obtained BRDF is publicly available as a part of our code package.

Figure 16 compares BRDFs and renderings the reference 3-axes material (the first column) with its automatic fitting (the second column) for three different illumination/viewing directions. As the parameters fitting is fully automatic, the user only has to provide information about the modes over-



Fig. 11 Comparison between reference BRDF (odd rows) and proposed BRDF model (even rows) renderings in *grace* illumination environment for 14 tested BRDFs

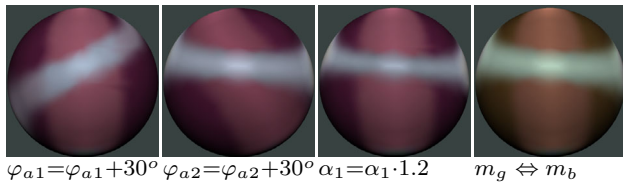


Fig. 12 Examples of BRDF anisotropy editing: **a** AHL1 shift 30°, **b** AHL2 shift 30°, **c** AHL1 width narrowed, **d** modes color parameters swapped

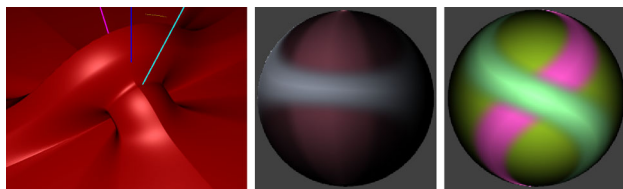


Fig. 13 Examples of our BRDF shader editing in BRDFExplorer: reflectance lobes, original fitted BRDF and its edit done in less than minute

lapping order and translucency (in this case $\beta_1 = 0, \beta_2 = 0$) needed at the merging step. Note that the color interpretation of our model is not perfect, and mainly due to the fact that the samples required for the model parameters estimation were also collected from overlapping areas of individual modes. To remedy this, we demonstrate the editing power of our model. We picked the representative color from the ref-

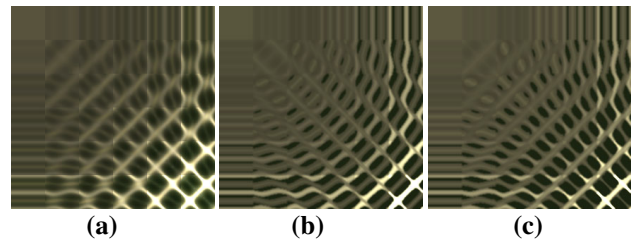


Fig. 14 Extension to retro-reflection highlights modeling: **a** reference BRDF, reconstructed BRDF **b** with anisotropic highlights, **c** with retro-reflective highlights

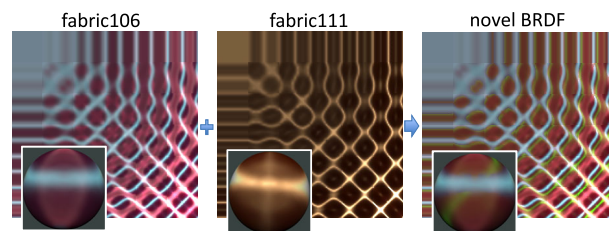


Fig. 15 Fabricating artificial BRDF with three distinct anisotropic modes, by combining BRDFs of *fabric106* and *fabric111* (applied as a 45° shifted *green highlight*)

erence BRDF for each anisotropy mode and used it instead of the originally estimated RGB parameters $m_{1,i}, m_{2,i}$. This resulted in a more vivid color reproduction as shown in the third column of Fig. 16. The fitted BRDF renderings in different illumination environments are shown in Fig. 17.

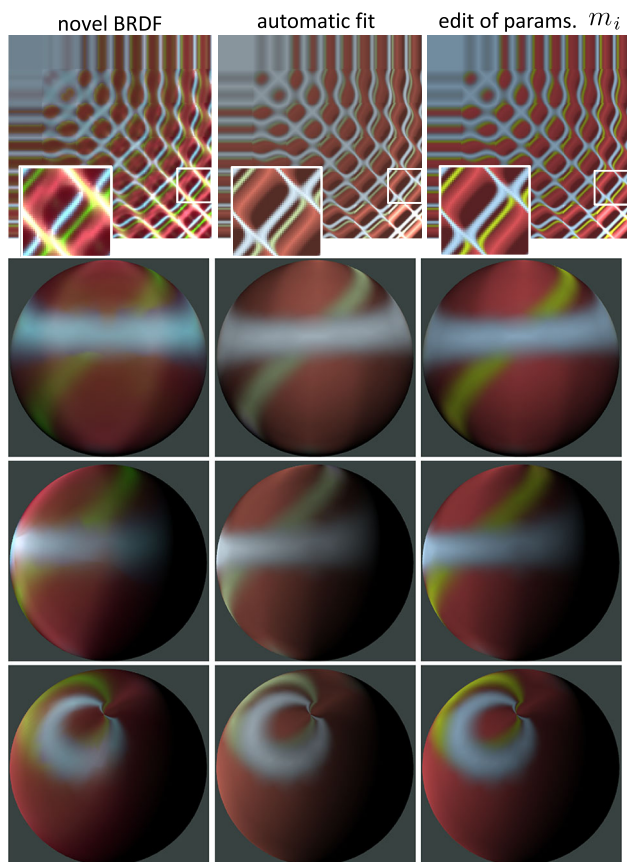


Fig. 16 Reconstruction and rendering of 3-axial BRDF. The *first column* shows generated reference BRDF, the *second column* shows the result of its automatic fitting, while its appearance after user edits of m_i is depicted in the *last column*

5.2 Limitations

The proposed modeling method naturally preserves reciprocity in BRDFs, while BRDF non-negativity is enforced. As for the majority of empirical models, energy conservation in BRDFs reconstructed by our method cannot be guaranteed due to possible inaccuracies in the specular component fitting.

A minor drawback in our approach is the requirement of a slight user intervention to adjust a global model's parameters (transparency β , highlights width w) so as to achieve optimal results. Also our current version of automatic parameters detection tends to shift color hue of the BRDF; however, the simple user control of parameters m_r , m_g , m_b can effectively remedy this (as shown in Fig. 16).

Usage of a current version of our model in Monte Carlo rendering schemes is limited due to a relatively complex nonlinear model equation. Therefore, the implementation of importance sampling remains a future endeavor of ours. Currently, our model can be applied in the Monte Carlo schemes only using precomputed factored BRDF representations [11].

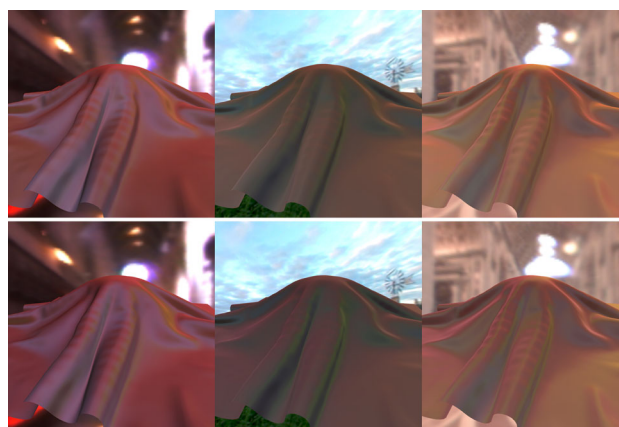


Fig. 17 Rendering of the fitted 3-axial BRDF in different illumination environments. The *first row* features the reference BRDF, while the *second row* shows its fitting by our model

6 Conclusions and future work

We present a novel empirical anisotropic BRDF model that fits individual modes of anisotropy independently using adaptive stencils of anisotropic highlights. Therefore, our approach does not need any time-demanding and potentially unstable numerical optimization. We tested performance on fourteen BRDFs exhibiting a wide range of anisotropic behavior. Our model allows for a very fast fitting, achieving robust results while simultaneously minimizing the need for user interaction. Furthermore, due to the independent fitting of individual modes of anisotropy, the proposed model allows for an intuitive editing of anisotropic appearance. Finally, we have shown that our model is appropriate for fast GPU rendering and can handle more than two anisotropy modes. Extension of our model for application in Monte Carlo importance sampling rendering schemes is a subject of our future work.

The BRDF fitting implementation in MATLAB and GPU shader for BRDFexplorer are publicly available.³

Acknowledgments We thank the anonymous reviewers for their insightful and inspiring comments. This research has been supported by the Czech Science Foundation Grant 14-02652S.

References

1. Ashikhmin, M., Shirley, P.: An anisotropic phong light reflection model. *J. Graph. Tools* **5**(2), 25–32 (2000)
2. Bagher Mahdi, M., Soler, C., Holzschuch, N.: Accurate fitting of measured reflectances using a Shifted Gamma micro-facet distribution. *Comput. Graph. Forum* **31**(4), 1509–1518 (2012)
3. Blinn, J.: Models of light reflection for computer synthesized pictures. *SIGGRAPH Comput. Graph.* **11**, 192–198 (1977)

³ <http://staff.utia.cz/filip/resources/stencils.zip>.

4. Cook, R., Torrance, K.: A reflectance model for computer graphics. *ACM SIGGRAPH Comput. Graph.* **15**(3), 307–316 (1981)
5. Dupuy, J., Heitz, E., Iehl, J., Poulin, P., Ostromoukhov, V.: Extracting microfacet-based BRDF parameters from arbitrary materials with power iterations. *Comput. Graph. Forum* **34**(4), 21–30 (2015)
6. Filip, J., Vavra, R.: Template-based sampling of anisotropic BRDFs. *Comput. Graph. Forum* **33**(7), 91–99 (2014)
7. He, X., Torrance, K., Sillion, F., Greenberg, D.: A comprehensive physical model for light reflection. *Comput. Graph.* **25**(4), 175–186 (1991)
8. Heitz, E.: Understanding the masking-shadowing function in microfacet-based BRDFs. *J. Comput. Graph. Tech. (JCGT)* **3**(2), 32–91 (2014)
9. Kurt, M., Szirmay-Kalos, L., Krivánek, J.: An anisotropic BRDF model for fitting and Monte Carlo rendering. *SIGGRAPH Comput. Graph.* **44**, 3:1–3:15 (2010)
10. Lafortune, E.P., Foo, S.C., Torrance, K.E., Greenberg, D.P.: Non-linear approximation of reflectance functions. *Comput. Graph.* **31**(Annual Conference Series), 117–126 (1997)
11. Lawrence, J., Rusinkiewicz, S., Ramamoorthi, R.: Efficient BRDF importance sampling using a factored representation. *ACM Trans. Graph.* **23**(3), 496–505 (2004)
12. Lu, R., Koenderink, J.J., Kappers, A.M.: Specularities on surfaces with tangential hairs or grooves. *Comput. Vis. Image Understand.* **78**(3), 320–335 (2000)
13. Nayar, S., Oren, M.: Generalization of the lambertian model and implications for machine vision. *Int. J. Comput. Vis.* **14**, 227–251 (1995)
14. Nicodemus, F., Richmond, J., Hsia, J., Ginsburg, I., Limperis, T.: Geometrical considerations and nomenclature for reflectance. *NBS Monograph* **160**, 1–52 (1977)
15. Pacanowski, R., Celis, O.S., Schlick, C., Granier, X., Poulin, P., Cuyt, A.: Rational BRDF. *IEEE Trans. Vis. Comput. Graph.* **18**(11), 1824–1835 (2012)
16. Phong, B.T.: Illumination for computer generated images. *Commun. ACM* **18**(6), 311–317 (1975)
17. Poulin, P., Fournier, A.: A model for anisotropic reflection. *SIGGRAPH Comput. Graph.* **24**(4), 273–282 (1990)
18. Raymond, B., Guennebaud, G., Barla, P., Pacanowski, R., Granier, X.: Optimizing BRDF orientations for the manipulation of anisotropic highlights. *Comput. Graph. Forum* **33**, 313–321 (2014)
19. Rusinkiewicz, S.: A new change of variables for efficient BRDF representation. In: *Rendering techniques' 98*, p. 11 (1998)
20. Sadeghi, I., Bisker, O., De Deken, J., Jensen, H.W.: A practical microcylinder appearance model for cloth rendering. *ACM Trans. Graph.* **32**(2), 14:1–14:12 (2013)
21. Schlick, C.: An inexpensive BRDF model for physically-based rendering. *Comput. Graph. Forum (EUROGRAPHICS'94)* **13**(3), 149–162 (1994)
22. Torrance, K., Sparrow, E.: Theory for off-specular reflection from rough surfaces. *J. Opt. Soc. Am.* **57**(9), 1105–1114 (1967)
23. Ward, G.: Measuring and modeling anisotropic reflection. *Comput. Graph.* **26**(2), 265–272 (1992)



Jiří Filip received the MSc and PhD, both in cybernetics from the Czech Technical University in Prague. Since 2002 he is a researcher at the Institute of Information Theory and Automation (UTIA) at the Czech Academy of Sciences. Between 2007 and 2009 he was Marie-Curie research fellow at Heriot-Watt University, Edinburgh. He combines methods of image processing, computer graphics, and visual psychophysics. His current research is focused on precise measurement, and modeling of material appearance.



Michal Havlíček received the MSc from the Czech Technical University in Prague. He currently works as a PhD candidate at Institute of Information Theory and Automation (UTIA) at the Czech Academy of Sciences. His research interest includes texture modeling and texture similarity.



Radomír Vávra received the MSc from the Czech Technical University in Prague. He currently works as a PhD candidate at Institute of Information Theory and Automation (UTIA) at the Czech Academy of Sciences. His research interest includes accurate material appearance measurement techniques and material visualization methods in computer graphics.